Hindawi Publishing Corporation
International Journal of Photoenergy
Volume 2013, Article ID 854857, 12 pages
http://dx.doi.org/10.1155/2013/854857

Research Article

Photodegradation of Rhodamine B Using the Microwave/UV/H_2O_2: Effect of Temperature

Carlo Ferrari,[1] H. Chen,[2,3] R. Lavezza,[4] C. Santinelli,[4] I. Longo,[1] and E. Bramanti[2]

[1] *INO, CNR Research Area of Pisa, Via G. Moruzzi 1, 56124 Pisa, Italy*
[2] *ICCOM, CNR Research Area of Pisa, Via G. Moruzzi 1, 56124 Pisa, Italy*
[3] *Department of Environmental Engineering, Civil & Environment Engineering School, University of Science and Technology, Beijing, 30 Xueyuan Road, Haidian, Beijing 100083, China*
[4] *IBF, CNR Research Area of Pisa, Via G. Moruzzi 1, 56124 Pisa, Italy*

Correspondence should be addressed to Carlo Ferrari; carlo.ferrari@ino.it

Received 11 January 2013; Accepted 17 July 2013

Academic Editor: Jafar Soltan

The oxidative decoloration of Rhodamine B (RhB) was performed in a photochemical reactor which enables microwave (MW) and UV radiation to be applied simultaneously. We used an immersed microwave source, with no need for an oven. Controlling the temperature, MW power, and UV emission of the reactor all led to a greater overall control of the process. Due to the action of highly reactive hydroxyl radicals, the decoloration of RhB was followed online using a spectrograph. Complete decoloration occurred in four minutes, and 92% of mineralisation was obtained in 70 minutes. The experiments were performed at various temperatures (21°C, 30°C, 37°C, and 46°C), with and without hydrogen peroxide. The apparent reaction rate was used to calculate the apparent activation energy of the decoloration process: $E_a = 38 \pm 2$ kJ/mol and 40 ± 2 kJ/mol with (400 mg/L) or without hydrogen peroxide, respectively. The lack of deviation from the linear behavior of the Arrhenius plot confirms that the application of MW does not affect the E_a of the process. The apparent activation energy value found was compared with the few data available in the literature, which were obtained in the absence of MW radiation and are inconsistent.

1. Introduction

The removal of dyes from industrial effluents has been receiving increasing attention, as legislation surrounding the release of contaminated effluents has become more stringent [1, 2]. Most textile dyes are photolytically stable and are specifically designed to resist fading upon exposure to sweat, sun light, water, and oxidizing agents [3]. These characteristics make them resistant to decomposition using conventional biochemical and physical-chemical methods.

Rhodamine B (RhB) is one of the most common xanthenes dyes used in the textile industry. This compound has now been banned from use in foods and cosmetics due to health hazards, that is, neurotoxicity and chronic toxicity in humans and animals [4]. Furthermore, RhB is a representative dye pollutant of industrial wastewater, which has often been used to develop or test new methods for the removal of recalcitrant species.

Considering its hazardous nature and harmful effects, it is important to remove RhB from wastewaters. For this purpose, generally adsorption on activated carbon, coagulation by a chemical agent, or reverse osmosis has been used [5, 6]. However, these are nondestructive methods, and merely transfer contaminants from water to sludge [7]. In addition, such contaminants are often highly toxic which means that biological treatments cannot be used, although they would be preferable in terms of the financial cost and energy consumption [2].

For the treatment of recalcitrant systems, as in the case of RhB, pretreatment can be performed using innovative methods, such as the Advanced Oxidation Process (AOP) and, more specifically, photochemical techniques [8]. These techniques could help to lower the toxicity of the molecules and reduce their size. In the literature, a large number of these methods have recently appeared. Many of them use ultraviolet radiation (UV), either on its own or in combination with

photocatalyzers [9], Fenton reactions [10], and other similar methods. Simple UV radiation can give rise to (i) direct photolysis of the pollutants [11] or (ii) indirect photolysis via a reactant generated from UV radiation, such as a hydroxyl radical generated by the presence of hydrogen peroxide [12, 13].

Recent articles have shown that RhB aqueous solutions can be decolorated using UV in the presence of hydrogen peroxide [7, 14–16]. The H_2O_2 shows a high molar absorption at 253 nm [17] and generates highly reactive hydroxyl radicals with a quantum yield near unity [18]:

$$H_2O_2 + h\nu \ (253\,\text{nm}) \longrightarrow 2HO\bullet \tag{1}$$

Since hydroxyl radicals are very strong oxidizing reagents, mainly through hydrogen extraction, they can react with the dye molecules to produce intermediates, which can cause a decoloration of the original solution [19]:

$$HO\bullet + \text{dye} \longrightarrow \text{intermediates} \longrightarrow CO_2 \uparrow + H_2O + \text{mineral salts} \tag{2}$$

Decoloration can be followed easily by measuring the absorbance at 554 nm using spectrophotometric techniques [3, 7, 14, 20–22].

Some authors report that the simultaneous application of microwave (MW) power and UV light leads to better results in photochemical processes [23–27]. Microwave radiation is often used for electrodeless lamps (EDLs), which have a longer life. To verify whether MW radiation really has a role in determining the value of the reaction rate and whether the UV/H_2O_2 method might be feasible in industry, it is necessary to compare the results with and without the presence of microwaves and measure the activation energy (E_a) of decoloration. In fact, E_a is the most important concept in chemical kinetics [28, 29] and is a necessary parameter for determining the reaction paths and designing industrial plants.

In a previous study by our research team, Longo and Ricci [30] proposed a novel fully integrated MW/UV photochemical reactor, which is easy to use, safe to handle, and reliable. The characteristic features and advantages of this reactor are reported in another one of our papers [31]. It appears to be suitable for continuous treatment and industrial scale-up [32]. The nonresonant microwave functioning of this photoreactor (cavity-less reactor) enabled us to fully control the physical parameters of the process, such as temperature, UV emission, and MW power. In addition, the MW power is supplied from the interior of the lamp and the reagents, in a reentrant lamp configuration [33], so that MW radiation is first used to produce the plasma discharge in the lamp, and it then propagates in the sample [34]. As a consequence, the UV emission depends on the MW power but to a very large extent not on the sample composition. This configuration leads to the best energy saving and to the most reliable experimental configuration. In fact, the MW power supplied to the lamp and to the reagents is controlled, is reproducible, and is easily measured, and there is no need to heat the sample to boiling. The UV emission of the lamp towards the sample is also controlled and reproducible.

In a resonant cavity such as an MW oven, on the other hand, the MW power is supplied by the exterior of the reagents, and the amount of MW power absorbed by the sample is unknown and cannot be controlled. In addition, in the case of an electrodeless lamp (EDL) immersed in the reagents, the MW power that reaches the lamp is unknown because it also depends, among many physical and geometric parameters (including the inhomogeneity of the electromagnetic field in the cavity), on the dielectric characteristics of the sample, which change during the course of treatment. Thus, as a consequence of the unknown shift in the dielectric properties of the sample, the UV emission (spectrum and intensity) is unknown and changes during the reaction. These experiments are usually carried out at the boiling temperature of the solution, which means that the activation energy E_a cannot be measured. All these factors make it impossible to measure the E_a of any process occurring in a resonant cavity or using devices involving common EDLs.

Our novel photoreactor overcomes all the drawbacks that commonly arise when EDLs are placed inside an MW oven [35]. In fact, we were able to perform experiments at a wide range of temperatures, at constant temperatures (in particular, below the solvent boiling point), and at a constant and controlled emission of the mercury EDLs (in particular, the UV line at 253 nm).

This study focuses on examining the oxidative decoloration of RhB, as a representative compound, by MW/UV/H_2O_2, through the following:

(1) the characterization of the UV source as a function of MW power and temperature,

(2) the optimization of H_2O_2 concentration,

(3) the determination of the apparent activation energy E_a of the decoloration, with and without added H_2O_2.

The measured E_a values of the decoloration were compared with those obtained by other researchers, using spectrophotometric measurements at 554 nm, on UV/H_2O_2 treatment without microwaves [20–22]. We believe that this is the first time that the apparent activation energy has been reported with microwave irradiation.

2. Materials and Methods

2.1. Photoreactor Apparatus. The photochemical reactor was made of quartz (type NHI 1101 high quality UV fused quartz, provided by Helios Italquartz, Milan, Italy: transmission > 85% from 180 nm to 4000 nm) and consisted of a flask containing a bulb filled with approximately 1 mg Hg and 0.66 kPa of Argon. The lamp bulb was fed from the interior by microwave power (2450 MHz) using a coaxial antenna probe (2.5 mm semirigid coaxial cable, Micro-Coax, Pottstown, PA, type UT 141, filled with PTFE). The open ended probe has a half-wave ($\lambda/2$) asymmetric dipole configuration, with λ being the wavelength of the MW radiation. The probe is constructed stripping off a $\lambda/4$ section of the external conductor of the semirigid 50 Ω coaxial cable.

The electromagnetic radiation delivered by the antenna, in particular the near field region, produces a gaseous plasma

discharge inside the bulb itself (Figure 1), the so-called microwave induced plasma (MIP) [33]. The bulb works at low pressure and low temperature, so that the energy transfer between the various chemical species of the plasma is not efficient, and the plasma is not in thermal equilibrium (non-LTE plasma) [33]. The recombination of the chemical species in the plasma (electrons and ions) produces the emission of electromagnetic radiation in a wide-frequency spectrum.

The UV emission is controlled by the MW power level. More MW power increases the number of excited molecules in the plasma and increases the amount of UV emission. The efficiency of the MW to UV conversion depends on the physical dimension of the bulb and on the pressure of the gas and the metal vapour filling the bulb. The fraction of microwaves not absorbed by the bulb propagates in the sample surrounding the bulb and is converted into heat.

The integrated MW/UV photoreactor is described in detail in Ferrari et al. [31] and has been used for degrading atrazine [36]. Figure 2 shows the experimental apparatus. The temperature is controlled by cooled tap water from a thermostat and allows isothermal measurements in the temperature range 10 ÷ 80°C (±0.5°C). The temperature of the solution inside the reactor is equilibrated using a magnetic stirrer. The spectral emission of the electrodeless lamp depends on the MW power and on the surface temperature. The MW power provided by the generator (Sairem, mod. GMP 03 K/SM) can be controlled manually or by RS232 remote control, up to 300 W. The stability of the temperature and the MW power supplied determine the stability of the UV emission.

Experiments to calculate the apparent activation energy of the decoloration of the RhB were carried out at different temperatures (T = 21°C, 30°C, 37°C, and 46°C) and required different MW power values in order to obtain the same UV emission. The calculation of the power required at each temperature (P = 77 W, 59 W, 46 W, and 35 W, resp.) was carried out on the basis of the data shown in Section 3.3. Each experiment was therefore carried out at a given temperature, each with the same UV radiation but with a different microwave irradiation.

The different microwave power irradiation determined the different amounts of energy released to the reagents and to the water matrix. However, this excess energy was removed by the cooling water because the experiments were conducted at a constant temperature. Any thermal effect related to the microwave irradiation was therefore removed.

Decoloration was followed online by a fiberoptic spectrograph (Avantes, Broomfield, CO, Mod. Ava Spec 3648-UA-50-AF) which measures the absorbance of the aqueous solution from 200 nm to 1000 nm using an immersed stainless steel probe.

In normal operating conditions, there is no emission of microwave radiation from the photoreactor, since the aqueous solution completely absorbs the MW. However, leakages of MW are potentially dangerous, so it is necessary to repeatedly monitor the various components of the experimental setup (coaxial cable, coaxial connectors, outside the photoreactor, etc.) with a microwave leakage detector (Robin, mod. TX90). Moreover, with the progress of the decolorization process, a greater amount of UV radiation escapes. For this reason, the eyes and skin should be protected.

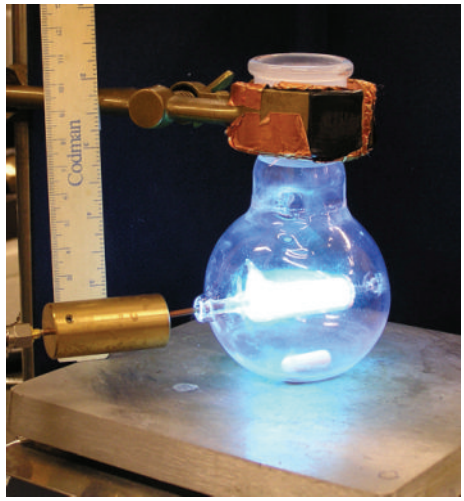

Figure 1: The MW/UV photoreactor. The quartz single-neck round flask, 200 mL capacity, houses the bulb. The recess in the bulb, which houses the coaxial antenna, consists of a quartz tube of internal diameter 3 mm and outer diameter 5 mm. The coaxial antenna is equipped with a cylindrical choke made of brass, with the length of 40 mm and external diameter of 20 mm.

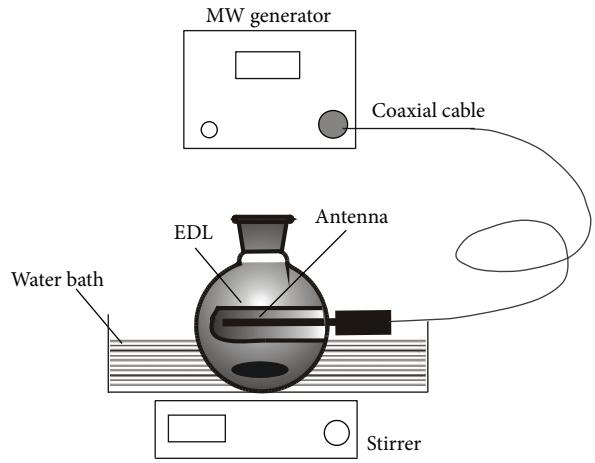

Figure 2: The experimental apparatus. The single-neck flask is soaked in a basin and is cooled by a water flow (pump and piping not shown, maximum flow of 1 L/min). The MW power is conveyed from the Sairem generator to the open coaxial antenna with a coaxial cable of 1 m.

2.2. Reagents. All chemicals were of the highest available purity. Rhodamine B (RhB, R-6626) was purchased from Sigma-Aldrich (Milan, Italy). Hydrogen peroxide (30% m/m solution) was obtained from Carlo Erba (Milan, Italy). HPLC-grade acetonitrile (ACN) and methanol from Carlo Erba were used. Distilled water was obtained using the Milli-Q water purification system (Millipore, Bedford, MA, USA). The stock solution was prepared freshly by dissolving RhB in Milli-Q water (10.2 mg/L). The photoreactor was filled with

120 mL of solution, and the desired amount of hydrogen peroxide was added.

2.3. High-Performance Liquid Chromatography (HPLC). The decoloration of RhB was monitored offline by high-performance liquid chromatography (HPLC) using a P4000 (Thermo Finnigan) equipped with a Rheodyne 7125 injector (Rheodyne, Cotati, CA, USA), a 20 μL poly(etheretherketone) (PEEK tubing, Upchurch, Oak Harbor, WA) injection loop and a UV6000 diode array detector (Thermo Finnigan). Separations were carried out using an MOS-2 Hypersil C18 (Thermo Fisher Scientific, UK) 250 × 2.1 mm column (silica particle size 5 μm) at room temperature (21 ± 1°C). The gradient elution of RhB and decoloration products was as follows: ACN/phosphate buffer (0.02 mol/L, pH 7) 1 : 99 for 4 min, then up to 60% ACN in 12 min, then up to 100% ACN in 2 min, and held for 12 min. The mobile phase flow was 0.2 mL/min. RhB was detected with a diode-array spectrophotometric detector at 544 nm.

2.4. Total Organic Carbon (TOC) Measurements. TOC measurements were carried out using a Shimadzu TOC-Vcsn Analyzer, equipped with a quartz combustion column filled with 1.2% Pt on alumina pillows of approximately 2 mm in diameter. The samples were automatically acidified with HCl Suprapur and purged for 3 min with high-pure air, in order to remove the inorganic carbon, before the high temperature catalytic oxidation [37]. One hundred mL of the sample was injected into the furnace after a fourfold rinse with the sample. From 3 to 5 replicate injections were performed until the analytical precision was within 2%.

A four-point calibration curve was created by injecting standard solutions (potassium hydrogen phthalate) in the same concentration ranges as the samples. The system blank was measured every day at the beginning and the end of the analysis using low-carbon water (2-3 μM) produced by a Milli-Q system. This low-carbon water was the same as the water used to prepare the standard solutions and was treated in the same way as the samples. TOC concentrations were calculated according to Thomas et al. [38], by the equation TOC = (Sample area − Blank area)/(slope of standard curve).

3. Results and Discussion

3.1. Effect of H_2O_2 Concentration. The primary aim of this study was to optimise the hydrogen peroxide concentration in order to obtain the maximum decoloration rate of RhB in the presence of MW and UV.

Figure 3 reports the absorbance spectra obtained at $T = 40^{\circ}$C and $P = 30$ W, with (Figure 3(b)) or without (Figure 3(a)) 300 mg/L of initial hydrogen peroxide. A value of 95% decoloration of RhB was reached within 3.5 and 10 min, with and without H_2O_2, respectively.

The shape of the spectra in the two cases (Figures 3(a) and 3(b)) is similar, although in the low wavelength side of the spectrum, absorption increased in the presence of hydrogen peroxide, and the decoloration was consistently faster.

The rate of decoloration was considerable even in the absence of H_2O_2. The decoloration was the same; however, the source of HO• radical was different. In fact, the homolysis of water was promoted in a restricted volume around the bulb, by the low wavelength line at 185 nm of the Hg spectrum [19, 39]:

$$H_2O + h\nu \ (<190\,\text{nm}) \longrightarrow H\bullet + HO\bullet \tag{3}$$

The relative emission at the 185 nm line varies between 5 to 10% of that at 253 nm, depending on the bulb's characteristics [19].

Direct UV decoloration of RhB can be ruled out, as no detectable degradation of RhB occurs by direct absorption of UV radiation at 253 nm [7], and direct decoloration of RhB from 185 nm is negligible compared to that caused by the interaction with HO• radicals [17].

Figure 4(a) shows the semilogarithmic plot of the absorbance value at 554 nm ($P = 30$ W and $T = 40^{\circ}$C) as a function of the time, at various initial hydrogen peroxide concentrations (0 ÷ 1800 mg/L). Assuming a pseudo-first-order reaction of the decoloration performed at a constant temperature, it is possible to obtain the apparent rate constant ($k_{1,554}$) using the absorbance value of the solution at the characteristic wavelength of the chromophore (554 nm). Indeed, no deviation from the first-order behaviour was observed in the conditions investigated.

The rate of reaction is well defined in simple reactions, where a single-reaction step occurs. In the case of complex reactions, it is still possible to define a reaction rate, which represents an average value between the constants in the reaction between different sites or different steps of the complex reaction, and is defined as the "apparent rate constant" [28, 40, 41].

The $k_{1,554}$ values obtained from the data in Figure 4(a) are reported in Figure 4(b) as a function of the initial hydrogen peroxide concentration, $[H_2O_2]_0$. The $k_{1,554}$ showed an increase in its values from 0.33 to 1.27 min^{-1} when the initial concentration of the H_2O_2 increased from 0 to 300 mg/L. For H_2O_2 concentrations higher than 400 mg/L, $k_{1,554}$ decreased until a value of 0.55 min^{-1} at 1800 mg/L of H_2O_2 due to the recombination of radical species and self-quenching of HO• radicals. The recombination of HO• radical and hydrogen peroxide produces $HO\bullet_2$ radicals [15], which are generally less effective than hydroxyl radicals [14]:

$$HO\bullet + H_2O_2 \longrightarrow HO\bullet_2 + H_2O \quad \left(k = 2.7 \times 10^7\ \text{M}^{-1}\,\text{s}^{-1}\right) \tag{4}$$

Generated hydroperoxyl radicals react to further reduce the HO• radical concentrations [7, 19]:

$$HO\bullet_2 + HO\bullet \longrightarrow H_2O + O_2 \quad \left(k = 6.6 \times 10^9\ \text{M}^{-1}\,\text{s}^{-1}\right) \tag{5}$$

On the basis of these results we chose an initial concentration of 400 mg/L H_2O_2 for the subsequent experiments, aimed at calculating the apparent activation energy of the RhB decoloration.

3.2. Total Organic Carbon (TOC) Measurements. The TOC concentration is commonly used to assess degradation, and

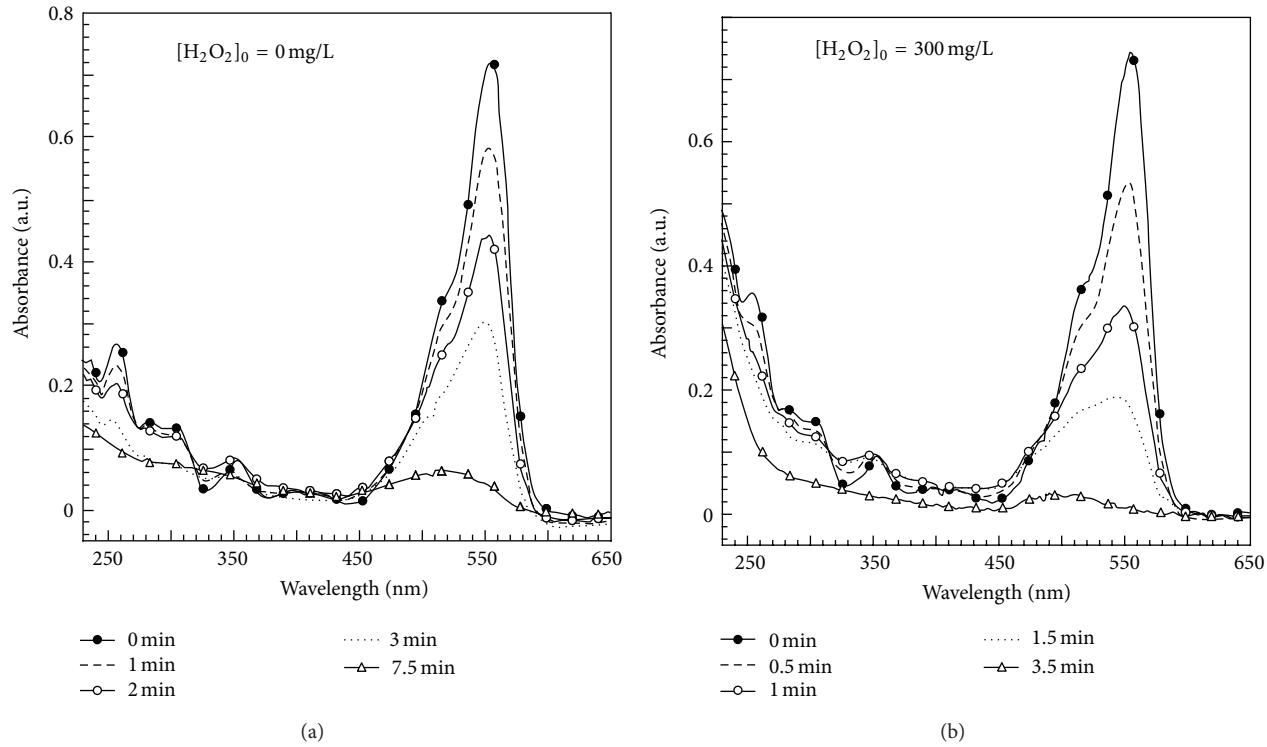

FIGURE 3: Absorbance spectra during the RhB (10.2 mg/L) decolorisation by MW + UV, without (a) and with (b) 300 mg/L hydrogen peroxide spiked in the solution. The power at the reactor's input was $P = 30 \pm 0.5$ W and $T = 40.0 \pm 1^{\circ}$C. Spectra were smoothed (boxcar = 10 points).

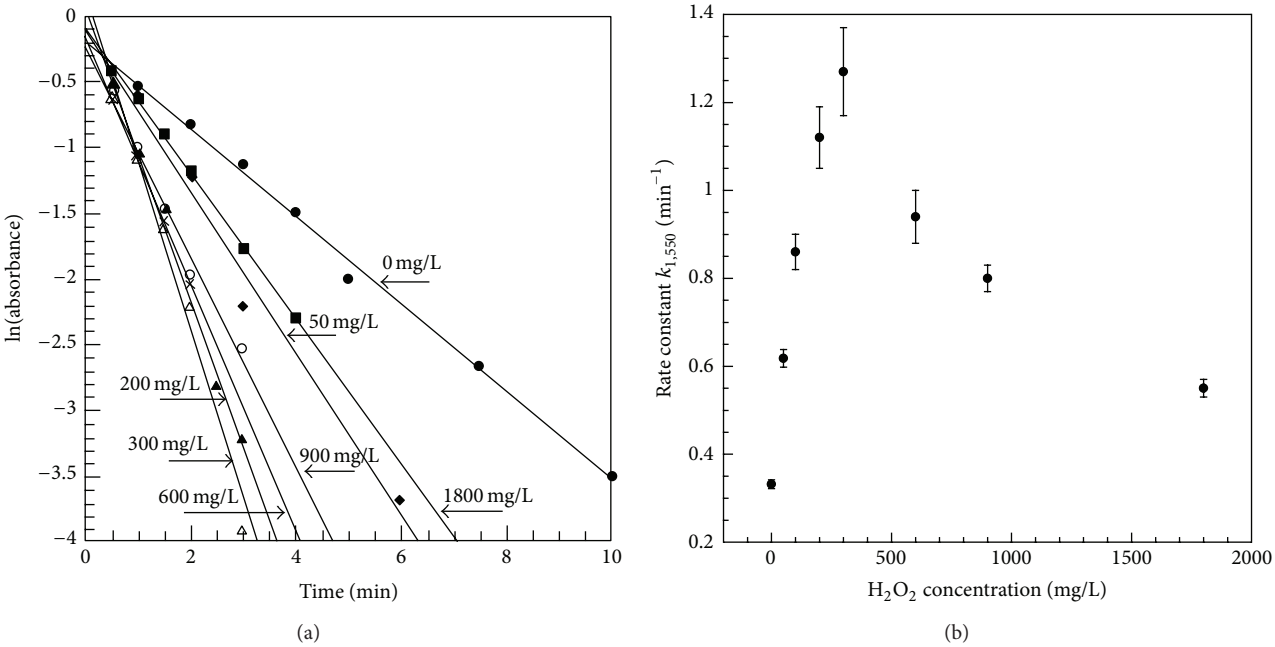

FIGURE 4: (a) Semilogarithmic plot of the absorbance of RhB solution (10.2 mg/L) at 554 nm versus time at various initial H_2O_2 concentrations, with $P = 30 \pm 0.5$ W and $T = 40 \pm 1^{\circ}$C (filled circles: 0 mg/L, filled diamonds: 50 mg/L, filled triangles: 200 mg/L, open triangles: 300 mg/L, crosses: 600 mg/L, open circles: 900 mg/L, and filled squares: 1800 mg/L). (b) Apparent rate constant $k_{1,554}$ of decoloration of RhB aqueous solution (10.2 mg/L) as a function of $[H_2O_2]_0$, with $P = 40 \pm 0.5$ W and $T = 40 \pm 1^{\circ}$C, obtained from data of (a).

some authors have found a close relationship between degradation and decolorization [7]. Although decoloration is a necessary step in the degradation process, determining the degradation path is very complex and requires a large number of measures and data in order to identify a reasonable number of chemical species. Thankfully, the exact determination of the degradation path is not relevant to this work because the activation energy is an empirical parameter that does not require any details of the physical-chemical process studied [28].

The TOC concentration was measured in RhB solutions with different initial additions of H_2O_2, collected after 4 min of irradiation, in order to evaluate the extent of RhB degradation in the various conditions. TOC showed a marked decrease, from 600 μM to 450 μM, in relation to an increasing concentration of H_2O_2 from 0 to 600 mg/L (Figure 5(a)). In contrast, in the RhB solution, after 4 min of irradiation, with an initial H_2O_2 concentration of 1800 mg/L, the TOC concentration showed values of 610 μM (Figure 5(a), curve (A)). These results confirm the trend of the apparent rate constant $k_{1,554}$ reported in Figure 4(b); that is, the maximum decoloration of RhB is obtained with an initial H_2O_2 addition between 300 and 600 mg/L (Figure 5(a), curve (B)). The data in Figure 5(a) prove that the decoloration, revealed by the apparent rate constant $k_{1,554}$ of absorbance, is closely related to the mineralization process revealed by the TOC content.

We also investigated the TOC concentrations of the RhB solution after different times of MW/UV irradiation in two conditions: with 0 and 400 mg/L of initial H_2O_2 concentrations (Figure 5(b)). The results showed a significant TOC decrease in the first 30 min of irradiation in both cases. However, the best result (50 μM TOC) was obtained after 70 min of irradiation in the sample with the addition of hydrogen peroxide (400 mg/L). In this case, the TOC was only 8% compared to its initial value (Figure 5(b)).

3.3. Characterization of the UV Emission. The bulb of the electrodeless lamp contains an inert gas (Ar) and a small amount of mercury. Both elements emit radiation when the plasma is activated inside the lamp by means of MW power. The emission of radiation by the rare gas in low-pressure EDL occurs if the partial pressure of mercury is sufficiently low. This condition is called "depleted discharge" [33] and is achieved when the temperature of the outer surface of the lamp is maintained at a low temperature, since the vapors of mercury condense on the walls of the lamp. The bulb containing the mixture of Ar and Hg produces a large number of emission lines between 185 nm and 950 nm (Figure 6). The radiation at 185 nm (UV-C radiation: 280–100 nm) is quickly absorbed by the sample or by air and is not detected by the spectrophotometer. The main emission in the UV-C region occurs at 253 nm. Two other emission lines are in regions UV-B (315–280 nm) and UV-A (400–315 nm), while the numerous remaining lines are in the visible or near-IR region. In a previous study, we demonstrated that the spectral emission of the electrodeless lamp depends on the MW power and on the temperature of the surface of the glass bulb [31].

Figure 6 shows two spectra obtained at different temperatures. A comparison between the two spectra revealed that, as the temperature increased, the short wavelength side of the spectrum, attributed to Hg, also increased. This behaviour could be explained by the increasing partial pressure of the Hg vapour in the bulb. In addition, the long wavelength side of the spectrum, attributed to Ar, decreased. The Ar emission depends on the mean free path of the free electron in the plasma: reducing the free path results in a reduction in the mean electron energy, which is progressively no longer sufficient to excite the atoms of rare gas.

The full characterization of the spectral emission of the electrodeless lamp is a prerequisite for performing experiments at different temperatures with the same UV irradiation and thus for calculating the activation energy of the process under investigation. The value of the UV radiation must remain constant because the molar absorptivity of the H_2O_2 changes very little as a function of temperature across the range examined here [42].

The spectral emission of the electrodeless lamp with pure water was collected under various MW powers (P = 15 W, 20 W, 25 W, 30 W, 35 W, and 40 W) and temperatures (T = 16.5°C, 29°C, 37°C, 46°C, and 54°C). Figure 7 reports the results of the 25 experiments collected at different temperatures and MW power. The three-dimensional plot reports the integrated area of the UV emission in the 250–256 nm range versus temperature and MW power. The combination of increasing temperature and increasing MW power produces a stronger emission in the UV region. On the basis of these data, using polynomial interpolation, we calculated various temperature-MW power couples for which the UV emission at 253 nm was constant (UV emission = 41000 ± 2000 Counts): 21°C and 77 W, 30°C and 59 W, 37°C and 46 W, 46°C and 35 W.

Table 1 reports the experimental conditions at the four different temperatures, with constant UV irradiation and various MW power. Table 1 also reports the estimated MW power not converted into visible light (column "power turned to heat") and absorbed by the water and subsequently converted into heat. The calculation takes into account that the conversion of microwave power to light radiation measured at high temperatures (lamp in air) is in the order of 23%. The estimate power released to the sample is very approximate. To carry out experiments at a controlled temperature, the thermal bath should remove the excess power released in the sample by the microwave radiation not converted into light.

3.4. Temperature Dependence Measurements. Designing a plant for the treatment of wastewater or developing a theoretical model requires knowledge of the relevant physical-chemical parameters. The temperature of the system, for example, influences the reaction kinetics. To be able to predict the behavior of the reaction and to establish appropriate operating parameters, the Arrhenius parameters need to be known as these determine the temperature dependence of the reaction. The activation energy value, in particular, is required and is defined unambiguously in the case of reactions consisting of a single step.

In the case of complex reactions, it is still possible to define an apparent activation energy E_a from the apparent rate of reaction [28, 40, 41]. In some cases, this parameter is

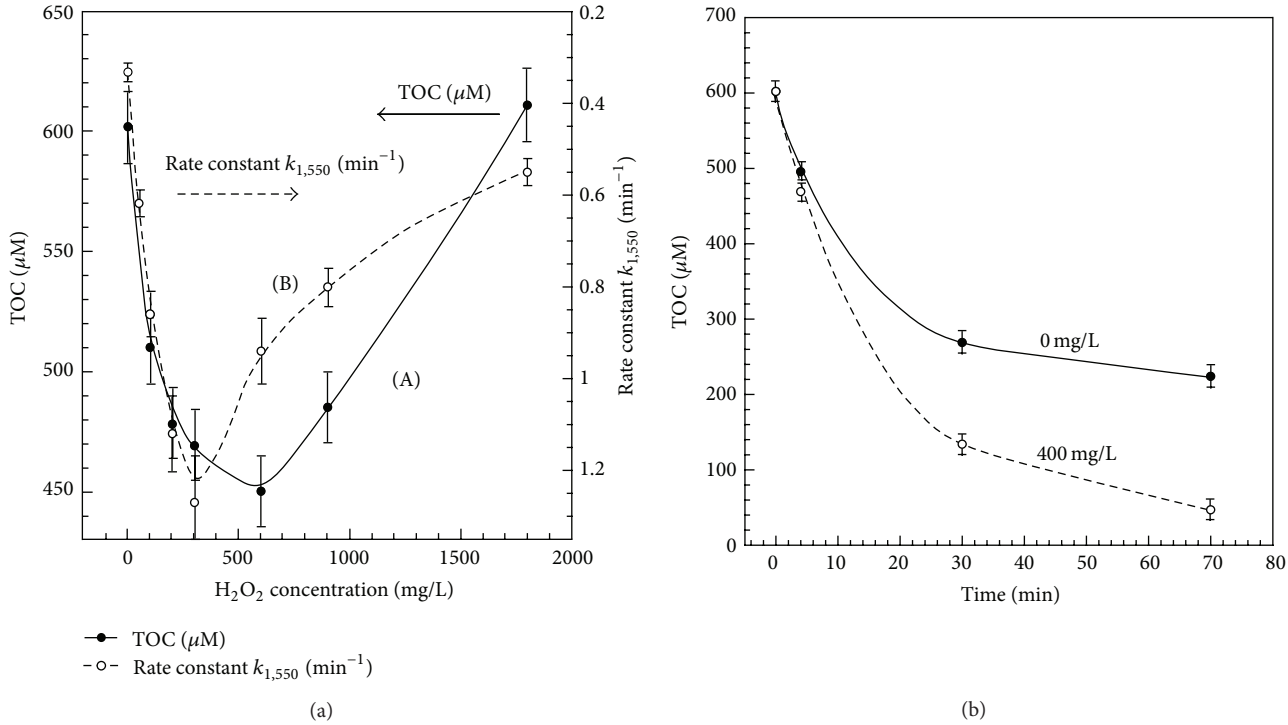

FIGURE 5: (a) Total organic carbon concentration (filled circles, curve (A), left scale) and apparent rate constant $k_{1,554}$ (open circles, curve (B), right scale) of RhB solution (10.2 mg/L) after 4 min of MW + UV irradiation ($P = 30 \pm 0.5$ W and $T = 40 \pm 1^{\circ}$C) versus $[H_2O_2]_0$. (b) Total organic carbon concentration of RhB aqueous solution (10.2 mg/L) as a function of irradiation time ($P = 30 \pm 0.5$ W and $T = 40 \pm 1^{\circ}$C) with $[H_2O_2]_0 = 400$ mg/L (open circles) and without (filled circles).

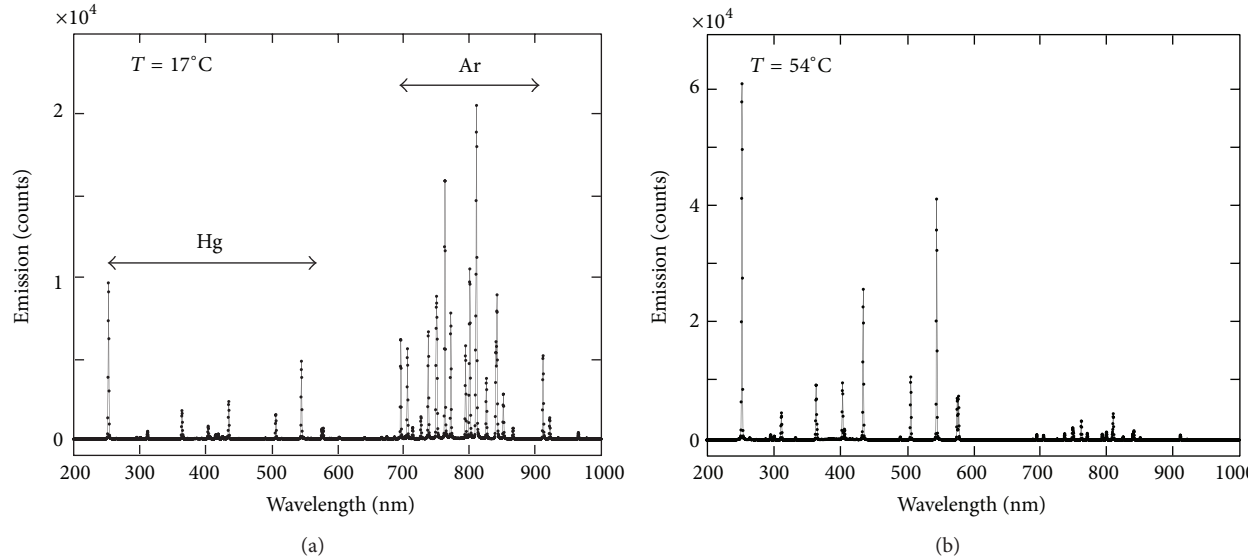

FIGURE 6: The emission spectrum of the integrated MW/UV lamp in the 200 ÷ 1000 nm region: (a) MW power = 40 W, $T = 17^{\circ}$C; (b) MW power = 40 W, $T = 54^{\circ}$C.

no longer a constant but depends on the temperature [28]. In such cases, it is possible to obtain information regarding the path of the chemical reaction or some other characteristics. For example, in competitive reactions in which a reagent A reacts to two different states B and C, with rate constant k_B and k_C, the total rate constant for the consumption of A, k_{TOT}, is then equal to $k_B + k_C$. If the two figures are significantly different, the E_a is strongly dependent on temperature. In general, the temperature dependence of the E_a arises if the rate constants of individual steps are combined additively.

Table 1: Experimental conditions at controlled temperatures and with the measured rate constant.

Photoreactor condition	T (°C)	UV (k Counts)	MW (W)	Power turned to heat (W)	$k_{1,554}$ (min^{-1}) $[H_2O_2]_0 = 0$ mg/L	$k_{1,554}$ (min^{-1}) $[H_2O_2]_0 = 400$ mg/L
1	21 ± 0.5	42 ± 2	77 ± 1	69 ± 5	0.12 ± 0.01	0.40 ± 0.01
2	30 ± 0.5	41 ± 1	59 ± 1	51 ± 5	0.17 ± 0.01	0.53 ± 0.01
3	37 ± 0.5	40 ± 1	46 ± 1	38 ± 5	0.28 ± 0.01	0.83 ± 0.01
4	46 ± 0.5	41 ± 1	35 ± 1	27 ± 5	0.42 ± 0.01	1.31 ± 0.01

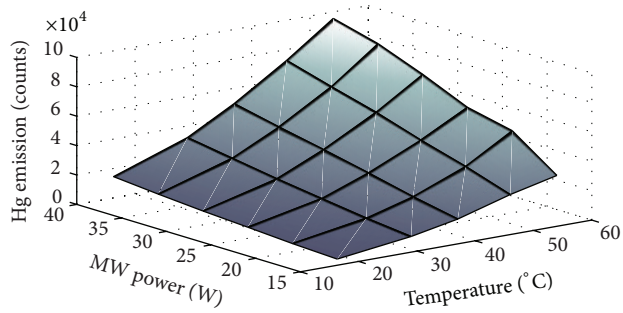

Figure 7: Three-dimensional plot of the integrated area of the UV emission line in the 250–256 nm range as a function of temperature and MW power.

Chemically, this means that some reactant or intermediate is partitioned between two different reaction pathways.

If, on the other hand, the overall rate constant is comprised of rate and equilibrium constants combined only through multiplication and division, the overall activation energy will essentially be independent of temperature. The overall (apparent) rate constant is the product of the rate constant of the individual steps. The overall (apparent) activation energy E_a is therefore independent of the temperature, unless the enthalpy component ΔH is dependent on the temperature [28].

Our case consists of at least two separate steps: the first, described by (1) (or (3)), in which the hydroxyl radicals are formed, and the second, described by (2), in which the HO• radicals react with the dye molecules. This second step may consist of competitive reactions or further steps. If competitive reactions are not possible, or if they have similar activation energies, the E_a will be a constant, independent of temperature [28]. In any case, the E_a of the overall process is the sum of the activation energies of the two consecutive steps:

$$E_a^{\text{TOT}} = E_a^{\text{Step 1 (HO• formation)}} + E_a^{\text{Step 2 (RhB decoloration)}}. \quad (6)$$

According to Minakata et al. [40], C–H bonds, –COOH functional group, aromatic rings, and –N<, which are present in the RhB molecule, can be the interaction sites of HO• radicals. Of these, only the loss of aromaticity is responsible for decoloration. For this reason, the occurrence of competitive reactions can thus be ruled out and E_a should be independent of temperature.

Experiments to determine the apparent activation energy must be conducted at various temperatures, with the same UV irradiation, as in the four operating conditions previously described in Section 3.3. The experimental conditions are summarized in Table 1. Figure 8 shows the semilogarithmic plot of the absorbance at 554 nm as a function of the irradiation time of the RhB solution with and without added hydrogen peroxide. The experimental data obtained were analysed to calculate the apparent rate constant of the RhB decoloration performed at a constant temperature, assuming a pseudo-first-order reaction, as reported in the last two columns of Table 1.

As expected, the apparent rate constant $k_{1,554}$ increases with the temperature. Figure 9 shows the apparent rate constant values obtained at various temperatures with (400 mg/L) or without (0 mg/L) hydrogen peroxide. The apparent activation energy was calculated according to the Arrhenius equation:

$$\ln(k_{1,554}) = -\frac{E_a}{kT} + \ln(A). \quad (7)$$

The E_a calculated was 38 ± 2 kJ/mol and 40 ± 2 kJ/mol with or without hydrogen peroxide, respectively (see Table 2). From the experimental measurements, no temperature dependence of the apparent activation energy had been inferred, within experimental error.

The contribution of the first step of (6) had been measured in a previous work [42], by means of photolysis experiments with radiation at 263 nm in aqueous solution, thus obtaining the value of approximately 6 kJ/mol. The contribution of the second step of (6) had also been calculated [40] and experimentally determined [44] only for simple aromatic compounds, ranging between 13 and 21 kJ/mol. Thus, the E_a calculated in this work is consistent with the values reported above.

Our experimentally measured E_a values were independent of the added hydrogen peroxide, within the experimental errors. Thus, it is possible to conclude that the activation energy of the two possible paths of the HO• formation, that is, (1) or (3), is the same within the experimental errors.

The similarity of the HPLC chromatograms of the RhB solution after the MW/UV process (data not shown) also confirmed that the by-products of MW/UV photodegradation with and without H_2O_2 were the same. This suggests that the decoloration path of the RhB was also the same, which is a further confirmation that the direct photolysis of the molecule of RhB provides a negligible contribution.

The apparent activation energy value found (38 ± 2 kJ/mol and 40 ± 2 kJ/mol) was consistent with the value calculated

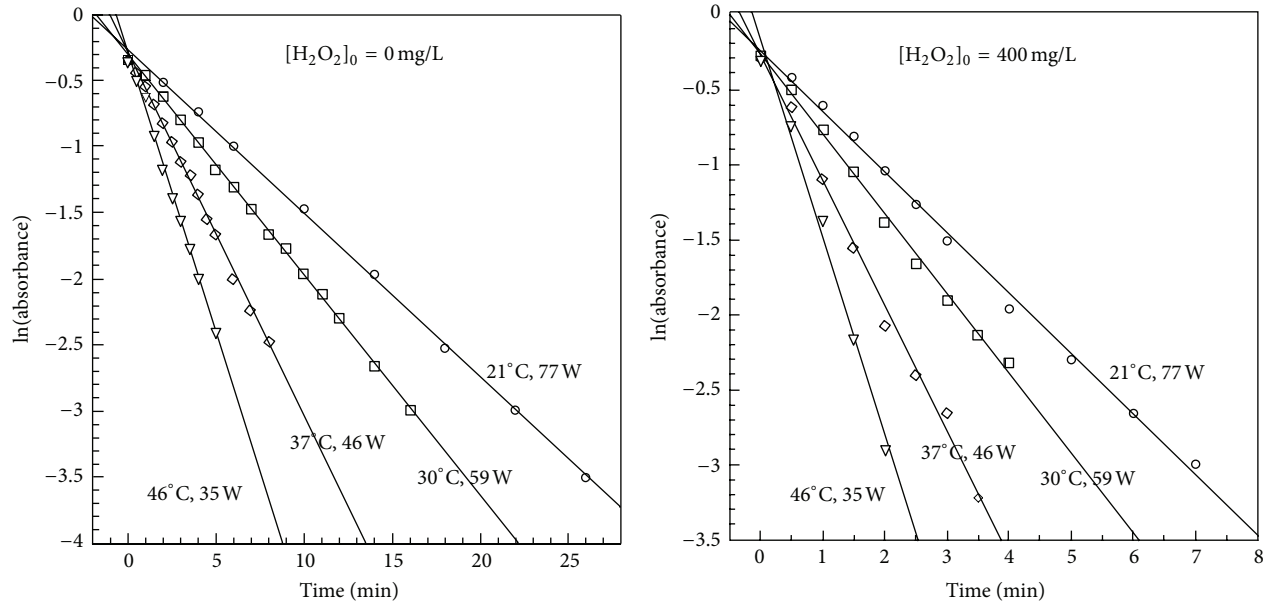

Figure 8: Semilogarithmic plot of the absorbance at 554 nm versus irradiation time of RhB solution (10.2 mg/L) without hydrogen peroxide (a) and with hydrogen peroxide (400 mg/L) (b), at various MW powers and temperatures (UV emission constant). Lines are the linear fitting of the ln(absorbance) data.

Table 2: The apparent activation energy results (kJ/mol).

Process and condition	UV (253 nm) + MW $[H_2O_2]_0 = 0$ mg/L	UV (253 nm) + MW $[H_2O_2]_0 = 400$ mg/L	UV (253 nm) $[H_2O_2]_0 = 200$ mg/L	UV (172 nm) $[H_2O_2]_0 = 0$ mg/L	UV (253 nm) + TiO_2 $[H_2O_2]_0 = 0$ mg/L	UV (263 nm) $[H_2O_2]_0 = 0$ mg/L
Decoloration of RhB	40 ± 2 [this work]	38 ± 2 [this work]	40.7 [22]	0 [43]	32.3 [20] 27.2 [21]	—
Water photolysis	—	—	—	—	—	6 [42]

by Mehrdad and Hashemzadeh [22] who used a UV/H_2O_2 system in the absence of MW: 40.7 kJ/mol. The E_a values found in our experiments are also higher than the UV/TiO_2 catalysed reaction, still without MW, reported by Byrappa et al. [20]: 32.3 kJ/mol, and Barka et al. [21]: 27.2 kJ/mol, as expected. Indeed, by definition, a catalyst provides a reaction path characterized by a lower activation energy. In contrast, Oppenländer and Xu [43] obtained different results using a flow photoreactor with UV irradiation at 172 nm, in which the HO• radicals were produced by water homolysis. They obtained a rate of reaction that was essentially independent of the temperature for the decolorisation of RhB; that is, basically the activation energy was zero. This result contrasts with both our data and other literature data and the E_a of the water homolysis (step 1 of the process), which has a value of approximately 6 kJ/mol. The contrasting outcome might be attributed to their experimental setup, in which the temperature control is limited to the container of the solution but does not include the volume in which the UV irradiation takes place.

Previous experimental results [23–27, 31] suggest that the use of MW in addition to the UV/H_2O_2 system obtains better yields in many reactions or reduces the treatment time of the decoloration. Our experimental results demonstrate that these improvements in chemical reactions, if any, are not caused by a decrease in activation energy. Therefore, the potential energy of reactants, products, and the activated complex at the transition state appear unchanged and unaltered by the MW application. In addition, our experiments were conducted with a different MW power level for each temperature (see Table 1, column 5: power turned to heat) and by removing the thermal effects of microwaves using circulation cooling water. It follows that if the application of MW significantly influenced the rate of reaction, then it should be possible to observe deviations from the linear behavior of the Arrhenius plot in Figure 9. Such deviations are not observable, within the experimental errors, which would seem to confirm that the application of microwaves does not influence the value of the apparent activation energy of the decoloration process.

3.5. Application and Energy Consumption. The novel photochemical reactor features a fully integrated MW+UV source for the in situ activation of a wide range of photochemical processes. Comparing it with the methods that currently use an MW oven [25–27], our photochemical reactor is much

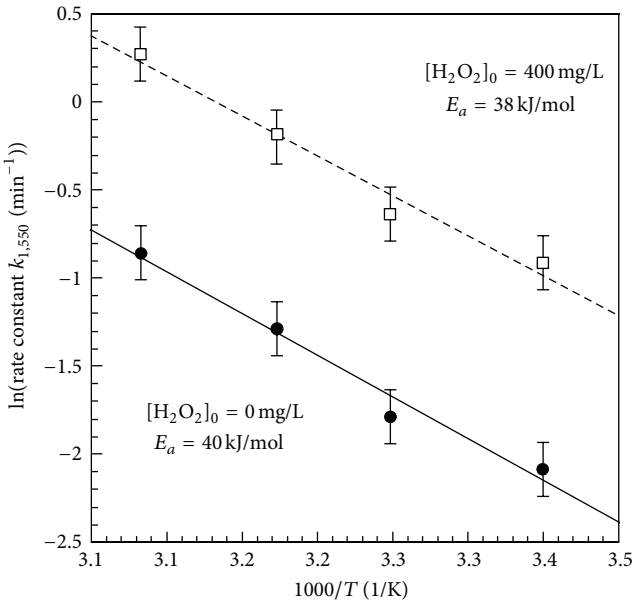

Figure 9: Arrhenius plot of the apparent rate constant of the RhB (10.2 mg/L) decoloration, assuming a pseudo, first, order reaction, with (open squares) and without (filled circles) hydrogen peroxide (400 mg/L). The apparent activation energy was calculated from the angular coefficient of the linear fitting curve.

more versatile and intrinsically more efficient for energy transfer, since, within limits, this transfer does not depend on the material and the geometry of the walls of the reaction vessel. It is therefore a good candidate for industrial applications.

As far as microwave activated photochemical processes are concerned, the major requirements the new method must satisfy to meet the needs of industrial applications are: (1) energy saving, (2) environmental benefits, (3) low cost, and most of all, (4) effective scalability.

Scalability can easily be obtained given that a number of modular integrated MW+UV applicators can be inserted in a vessel of whatever size and wall material, to energize a process at power levels of many kW of MW and UV power, with the electronic control of the power emitted by each applicator. We recently tackled problem of antenna cooling, and it was solved in the case of continuous processes with flowing aqueous reactants and will be described in a separate article.

A nonexhaustive list of potential industrial needs and includes the following applications of this technology.

(i) Microwave advanced oxidation, (ii) UV treatment of microorganism contaminated materials, (iii) water disinfection, (iv) decoloration of effluent from tanneries or textile dyeing, (v) MW and UV activated photochemistry and photocatalysis, (vi) nanoparticle preparation by photo-reduction, and (vii) high power UV photo-induced polymerisation.

The electrical energy consumption (E_{EO}) is the figure of merit for situations where the pollutant concentration is low (generally pseudo-first-order reactions) and is the electric energy in kilowatt hours required to degrade a contaminant by one order of magnitude in a unit volume of contaminated water (kWh/m^3/order) [45]:

$$E_{EO} = \frac{1000Pt}{V \log\left(c_i/c_f\right)} = \frac{38.4P}{Vk_{1,550}}, \quad (8)$$

where P is the electric power (kW), V is the volume (L) of water treated in the time t (h), c_i, c_f are the initial and final concentrations of pollutant, and $k_{1,550}$ is the first-order rate constant (min^{-1}). The value of E_{EO} is strongly influenced by the efficiency of the UV lamp. The greater the efficiency of conversion from radiation MW to UV radiation, the lower the energy consumption and thus the lower the E_{EO}. In our case, the reentrant configuration allows the highest efficiency. In addition, it is possible to increase the volume of the bulb in order to increase the conversion efficiency. It is important to note, however, that in order to avoid self-absorption the plasma must occupy the entire volume of the bulb.

In our best case (T = 46°C, P = 35 W, with 400 mg/L spiked H_2O_2, $k_{1,550}$ = 1.31, V = 0.12 L) the E_{EO} resulted in an 8.5 kWh/m^3/order. This value is consistent with the values reported by other authors under similar conditions [6]. It enables the industry and potential users to have a standardized objective basis for comparison and is useful for a system cost estimation [45].

4. Conclusions

We have described the application of a novel photochemical reactor to the oxidative decoloration of Rhodamine B dye by MW/UV/H_2O_2. The complete control of all the relevant parameters of the reactor (temperature, MW power, and UV emission) led to a greater and more realistic knowledge of the energetic aspects of the process. For what we believe is the first time, it was possible to measure the apparent activation energy of the decoloration process in the presence of MW, with and without hydrogen peroxide. The E_a was found to be independent of the addition of hydrogen peroxide. The apparent activation energy value was also consistent with the value obtained by other authors without MW. The lack of deviations from the linear behavior of the Arrhenius plot confirms that the application of MW does not affect the apparent reaction rate of the decoloration of RhB. The results obtained in this study could be easily extended to other photochemical processes. The photoreactor may be suitable for the characterization of photochemical processes in controlled conditions and for easy, low-cost, and "green" (no chemicals added) pretreatments of wastewaters.

Acknowledgments

The authors are grateful to the Italian Ministry for University and Research for the financial support. The work was supported by MIUR Grant PRIN 2008, prot. 2008SXASBC_003. Huilun Chen would like to acknowledge financial support from the Chinese Scholarship Council (CSC). The authors would like to thank C. Lanza and F. Pardini (INO-CNR) for their valuable technical support.

References

[1] X. Wang, J. Wang, P. Guo, W. Guo, and C. Wang, "Degradation of rhodamine B in aqueous solution by using swirling jet-induced cavitation combined with H_2O_2," *Journal of Hazardous Materials*, vol. 169, no. 1–3, pp. 486–491, 2009.

[2] S. Vilhunen and M. Sillanpää, "Recent developments in photochemical and chemical AOPs in water treatment: a mini-review," *Reviews in Environmental Science and Biotechnology*, vol. 9, no. 4, pp. 323–330, 2010.

[3] I. Arslan and I. A. Balcioglu, "Degradation of Remazol Black B dye and its simulated dyebath wastewater by advanced oxidation processes in heterogeneous and homogeneous media," *Coloration Technology*, vol. 117, no. 1, pp. 38–42, 2001.

[4] D. Kornbrust and T. Barfknecht, "Testing Dyes in HPC/DR systems," *Environmental Mutagenesis*, vol. 7, pp. 101–120, 1985.

[5] L. Young and J. Yu, "Ligninase-catalysed decolorization of synthetic dyes," *Water Research*, vol. 31, no. 5, pp. 1187–1193, 1997.

[6] N. Daneshvar, H. Ashassi-Sorkhabi, and A. Tizpar, "Decolorization of orange II by electrocoagulation method," *Separation and Purification Technology*, vol. 31, no. 2, pp. 153–162, 2003.

[7] N. Daneshvar, M. A. Behnajady, M. K. A. Mohammadi, and M. S. S. Dorraji, "UV/H_2O_2 treatment of Rhodamine B in aqueous solution: influence of operational parameters and kinetic modeling," *Desalination*, vol. 230, no. 1–3, pp. 16–26, 2008.

[8] Z. L. Ye, C. Q. Cao, J. C. He, R. X. Zhang, and H. Q. Hou, "Photolysis of organic pollutants in wastewater with 206 nm UV irradiation," *Chinese Chemical Letters*, vol. 20, no. 6, pp. 706–710, 2009.

[9] R. Mohammadi, B. Massoumi, and M. Rabani, "Photocatalytic decomposition of amoxicillin trihydrate antibiotic in aqueous solutions under UV irradiation using Sn/TiO_2 Nanoparticles," *International Journal of Photoenergy*, vol. 2012, Article ID 514856, 11 pages, 2012.

[10] C. Benincá, P. Peralta-Zamora, R. C. Camargo, C. R. G. Tavares, E. F. Zanoelo, and L. Igarashi-Mafra, "Kinetics of oxidation of ponceau 4R in aqueous solutions by Fenton and photo-Fenton processes," *Reaction Kinetics, Mechanisms and Catalysis*, vol. 105, pp. 293–306, 2011.

[11] G. Matafanova and V. Batoev, "Recent progress on application of UV excilamps for degradation of organic pollutants and microbial inactivation," *Chemosphere*, vol. 89, pp. 637–647, 2012.

[12] D. H. Tseng, L. C. Juang, and H. H. Huang, "Effect of Oxygen and Hydrogen peroxide on the photocatalytic degradation of monoclhorobenzene in TiO_2 aqueous suspension," *International Journal of Photoenergy*, vol. 2012, Article ID 328526, 9 pages, 2012.

[13] C.-M. Ma, G.-B. Hong, H.-W. Chen, N.-T. Hang, and Y.-S. Shen, "Photooxidation contribution study on the decomposition of azo dyes in aqueous solutions by VUV-based AOPs," *International Journal of Photoenergy*, vol. 2011, Article ID 156456, 8 pages, 2011.

[14] F. H. AlHamedi, M. A. Rauf, and S. S. Ashraf, "Degradation studies of Rhodamine B in the presence of UV/H_2O_2," *Desalination*, vol. 238, no. 1–3, pp. 159–166, 2009.

[15] V. V. Goncharuk, N. M. Soboleva, and A. A. Nosonovich, "Photooxidative destruction of organic compounds by hydrogen peroxide in water," *Journal of Water Chemistry and Technology*, vol. 32, no. 1, pp. 17–32, 2010.

[16] S. Yang, Y. Huang, Y. Wang, Y. Yang, M. Xu, and G. Wang, "Photocatalytic degradation of Rhodamine B with $H_3PW_{12}O_{40}$/SiO_2 sensitized by H_2O_2," *International Journal of Photoenergy*, vol. 2012, Article ID 927132, 6 pages, 2012.

[17] O. Legrini, E. Oliveros, and A. M. Braun, "Photochemical processes for water treatment," *Chemical Reviews*, vol. 93, no. 2, pp. 671–698, 1993.

[18] P. K. Malik and S. K. Sanyal, "Kinetics of decolourisation of azo dyes in wastewater by UV/H_2O_2 process," *Separation and Purification Technology*, vol. 36, no. 3, pp. 167–175, 2004.

[19] M. G. Gonzalez, E. Oliveros, M. Wörner, and A. M. Braun, "Vacuum-ultraviolet photolysis of aqueous reaction systems," *Journal of Photochemistry and Photobiology C*, vol. 5, no. 3, pp. 225–246, 2004.

[20] K. Byrappa, A. K. Subramani, S. Ananda, K. M. Lokanatha Rai, R. Dinesh, and M. Yoshimura, "Photocatalytic degradation of rhodamine B dye using hydrothermally synthesized ZnO," *Bulletin of Materials Science*, vol. 29, no. 5, pp. 433–438, 2006.

[21] N. Barka, S. Qourzal, A. Assabbane, A. Nounah, and Y. Ait-Ichou, "Factors influencing the photocatalytic degradation of Rhodamine B by TiO_2-coated non-woven paper," *Journal of Photochemistry and Photobiology A*, vol. 195, no. 2-3, pp. 346–351, 2008.

[22] A. Mehrdad and R. Hashemzadeh, "Determination of activation energy for the degradation of rhodamine B in the presence of hydrogen peroxide and some metal oxide," *Journal of the Chemical Society of Pakistan*, vol. 31, no. 5, pp. 738–743, 2009.

[23] S. Chemat, A. Aouabed, P. V. Bartels, D. C. Esveld, F. Chemat, and E. Esveld, "Original microwave-ultraviolet combined reactor suitable for organic synthesis and degradation," *Journal of Microwave Power and Electromagnetic Energy*, vol. 34, no. 1, pp. 55–60, 1999.

[24] V. Církva and M. Hájek, "Microwave photochemistry. Photoinitiated radical addition of tetrahydrofuran to perfluorohexylethene under microwave irradiation," *Journal of Photochemistry and Photobiology A*, vol. 123, no. 1–3, pp. 21–23, 1999.

[25] P. Klán, J. Literák, and M. Hájek, "The electrodeless discharge lamp: a prospective tool for photochemistry," *Journal of Photochemistry and Photobiology A*, vol. 128, pp. 145–149, 1999.

[26] S. Horikoshi, H. Hidaka, and N. Serpone, "Environmental remediation by an integrated microwave/UV-illumination method. 1. Microwave-assisted degradation of rhodamine-B dye in aqueous TiO_2 dispersions," *Environmental Science and Technology*, vol. 36, no. 6, pp. 1357–1366, 2002.

[27] S. Horikoshi, A. Saitou, H. Hidaka, and N. Serpone, "Environmental remediation by an integrated microwave/UV-illumination method. 5. Thermal and non-thermal effects of microwave radiation on the photocatalyst and on the photodegradation of rhodamine-B dye under UV/Visible radiation," *Environmental Science and Technology*, vol. 37, no. 24, pp. 5813–5822, 2003.

[28] J. F. Bunnett, "The interpretation of rate data," in *Technique of Organic Chemistry*, A. Weissberger, Ed., vol. VIII, Part I of *Investigation of Rates and Mechanism of Reactions*, pp. 177–283, Interscience Publishers, London, UK, 1961.

[29] M. M. Rahman, R. Saha, B. Ahmed et al., "Light induced kinetic studies of oxidative degradation of malachite green," *Asian Journal of Chemistry*, vol. 23, no. 3, pp. 945–949, 2011.

[30] I. Longo and A. S. Ricci, "Chemical activation using an open-end coaxial applicator," *Journal of Microwave Power and Electromagnetic Energy*, vol. 41, no. 1, pp. 4–19, 2007.

[31] C. Ferrari, I. Longo, E. Tombari, and E. Bramanti, "A novel microwave photochemical reactor for the oxidative decomposition of Acid Orange 7 azo dye by MW/UV/H_2O_2 process,"

Journal of Photochemistry and Photobiology A, vol. 204, no. 2-3, pp. 115–121, 2009.

[32] C. Ferrari, I. Longo, E. Tombari, and L. Gasperini, "A new integrated photoreactor for microwave assisted decolorization of Acid Orange 7 (AO7) in aqueous solutions," *International Journal of Chemical Reactor Engineering*, vol. 8, article A72, 2010.

[33] A. Bogaerts, E. Neyts, R. Gijbels, and J. Van der Mullen, "Gas discharge plasmas and their applications," *Spectrochimica Acta B*, vol. 57, no. 4, pp. 609–658, 2002.

[34] I. Longo, "Method for the production of a Visible, UV or IR radiation with a lamp without electrodes and lamp that carries out this method," European Patent Application PCT/IB02/05004, 2004.

[35] V. Církva and S. Relich, "Microwave photochemistry and photocatalysis. part 1: principles and overview," *Current Organic Chemistry*, vol. 15, no. 2, pp. 248–264, 2011.

[36] H. Chen, E. Bramanti, I. Longo, M. Onor, and C. Ferrari, "Oxidative decomposition of atrazine in water in the presence of hydrogen peroxide using an innovative microwave photochemical reactor," *Journal of Hazardous Materials*, vol. 186, no. 2-3, pp. 1808–1815, 2011.

[37] P. J. L. Williams, J. Bauer, R. Benner et al., "Measurement of dissolved organic-carbon and nitrogen in natural-waters—doc subgroup report," *Marine Chemistry*, vol. 41, no. 1–3, pp. 11–21, 1993.

[38] C. Thomas, G. Cauwet, and J. F. Minster, "Dissolved organic carbon in the equatorial Atlantic Ocean," *Marine Chemistry*, vol. 49, no. 2-3, pp. 155–169, 1995.

[39] J. K. Thomas and E. J. Hart, "Photolysis and radiolysis of aqueous solutions at high radiation intensities," *Journal of Physical Chemistry*, vol. 68, no. 9, pp. 2414–2418, 1964.

[40] D. Minakata, K. Li, P. Westerhoff, and J. Crittenden, "Development of a group contribution method to predict aqueous phase hydroxyl radical (HO•) reaction rate constants," *Environmental Science and Technology*, vol. 43, no. 16, pp. 6220–6227, 2009.

[41] G. McKay, M. M. Dong, J. L. Kleinman, S. P. Mezyk, and F. L. Rosario-Ortiz, "Temperature dependence of the reaction between the hydroxyl radical and organic matter," *Environmental Science and Technology*, vol. 45, no. 16, pp. 6932–6937, 2011.

[42] L. Chu and C. Anastasio, "Formation of hydroxyl radical from the photolysis of frozen hydrogen peroxide," *Journal of Physical Chemistry A*, vol. 109, no. 28, pp. 6264–6271, 2005.

[43] T. Oppenländer and F. Xu, "Temperature effects on the vacuum-UV (VUV)-initiated oxidation and mineralization of organic compounds in aqueous solution using a xenon excimer flow-through photoreactor at 172 nm," *Ozone*, vol. 30, no. 1, pp. 99–104, 2008.

[44] L. Ashton, G. V. Buxton, and C. R. Stuart, "Temperature dependence of the rate of reaction of OH with some aromatic compounds in aqueous solution. Evidence for the formation of a π-complex intermediate?" *Journal of the Chemical Society, Faraday Transactions*, vol. 91, no. 11, pp. 1631–1633, 1995.

[45] J. R. Bolton, K. G. Bircher, W. Tumas, and C. A. Tolman, "Figures-of-merit for the technical development and application of advanced oxidation technologies for both electric- and solar-driven systems—(IUPAC Technical Report)," *Pure and Applied Chemistry*, vol. 73, no. 4, pp. 627–637, 2001.